

A V2G-enabled Seven-level Buck PFC Rectifier for EV Charging Application

Anekant Jain, Ritika Agarwal, Krishna Kumar Gupta, Sanjay K. Jain

Thapar Institute of Engineering and Technology,
Patiala, India

E-Mail: ajain_phd19@thapar.edu, ritikaagarwal290@gmail.com,
krishna.gupta@thapar.edu, skjain@thapar.edu

Keywords

« AC-DC converter », «Charging infrastructure for EV's », « Electric vehicle », « Multi-level converters », « Power factor correction ».

Abstract

This article presents a novel bidirectional multilevel buck rectifier with power factor correction for the charging systems of currently available commercialized electric vehicles. As it synthesizes seven voltage levels, the proposed rectifier entails low harmonics. This rectifier enables grid-to-vehicle (G2V) operation in buck mode and vehicle-to-grid (V2G) operation in boost mode. The proposed topology utilizes the switched capacitors principle to achieve a self-voltage balancing of the capacitors. Experimental results are presented to validate the proposed rectifier.

Introduction

The most significant innovation in the automobile industry is the electric vehicle (EV). Electric vehicles are gaining popularity these days at an exponential rate. As a result of this expansion, more energy-efficient charging infrastructure is needed[1]. EVs provide several advantages: environmental preservation, lower running costs, zero tailpipe emission, no noise pollution and more convenient. EVs may act as a load i.e., grid-to-vehicle (G2V) and as a generator i.e., vehicle-to-grid (V2G) modes [2], [3]. As the power of a typical EV is double that of the normal residential load and fast charging will impose pressure on the grid network. If the EV charging does not employ state-of-the-art conversion, grid disruptions occur such as undesirable peak loads, harmonics, and poor power factor may occur [4]. To overcome this problem, a V2G technology refers to the process of feeding the electricity contained in an electric car's batteries back into the electrical grid. As a result, the V2G technology makes energy injection back into the grid easier. This technology forms part of a smart grid, an electrical network system that uses information technology to manage energy consumption. In general, the power converter is unidirectional for G2V mode, which includes both onboard and off-board charging systems. To enable V2G mode the grid-connected bidirectional AC-DC converter is required, which can provide sinusoidal input current with a unity power factor (UPF)[5]. The main research directions for bidirectional AC-DC converters are increasing power density, minimizing input and output current ripple, maintaining UPF and offering power adjustment capability.

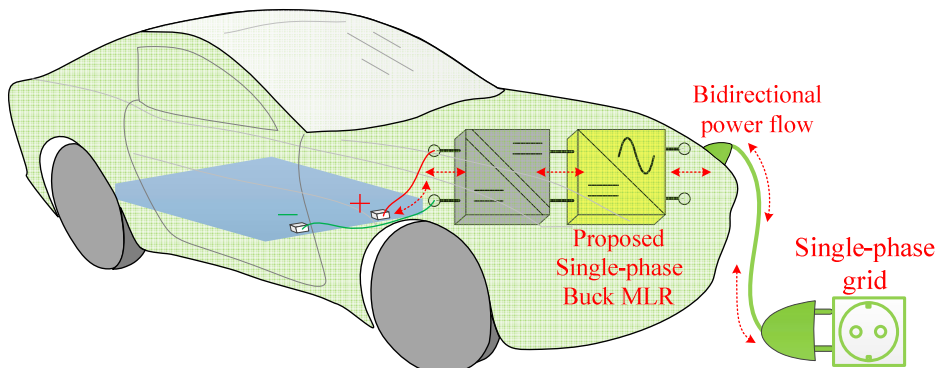


Fig. 1: Schematic diagram of the proposed charging system.

This article is focused on V2G enabled bidirectional single-phase on-board EV charging system. The design and development of this work can charge the vehicle battery as well as offer active power support to the utility grid as described in this article[6]. Fig. 1 depicts a schematic diagram of the proposed charging system, which is divided into two stages; first one is the bidirectional PFC converter and second is bidirectional DC-DC converter.

A conventional AC-DC converter converts the incoming AC grid voltage into a regulated boost DC link voltage[7]. A high voltage DC-DC buck converter is necessary to reduce this voltage to the nominal voltage acceptable for EV battery charging[8]. In this setup, the total standing voltage (TSV) between the rectifier and DC-DC converter switches is equal to the DC-link voltage i.e., high. Moreover, it required a high-voltage DC-bus capacitor [9]. The use of buck PFC rectification can fix these difficulties [10]. However, this results in discontinuous conduction mode (DCM), requiring larger inductive and capacitive filters on both DC and AC sides[11],[12]. Furthermore, DCM topologies' high-frequency operation considerably increases the switching losses. A diode bridge and a DC-DC buck converter are other ways to generate a buck DC voltage. Such two-stage systems have poorer efficiency, increased power losses, and higher production costs for medium and high-power applications[13].

A multilevel rectifier (MLR) is a revolutionary technology that can allow bidirectional power transfer. Compared to two-level converters, these converters employ lower-rated power switches, resulting in a higher-quality voltage waveform, less dv/dt stress across the switches, and lower THD line current[14]. As a result, of high-power applications, the power losses and the filter size decrease. In the AC-DC conversion of the EV charging system, conventional MLRs topologies, including neutral point clamped, flying capacitor, and T-type, have been used to enhance output voltage conversion [14]–[16]. These MLRs, on the other hand, have the following flaws:

- This functioned as a boost mode.
- The boost DC output voltage equalizes the blocking voltage on power switches.
- As the voltage level rises, the number of capacitors also rises, requiring more complex control techniques to balance the voltages of the capacitors.
- A high DC-bus capacitor is required.

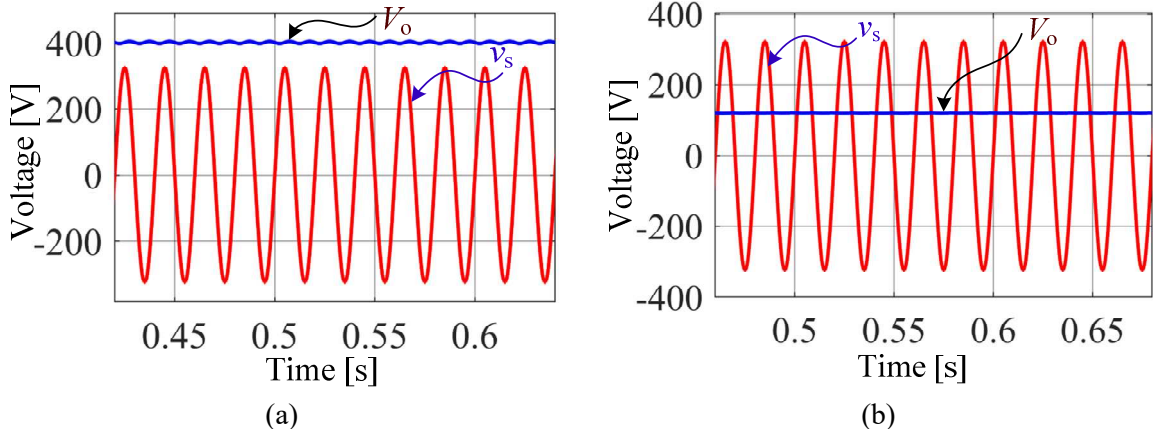


Fig. 2: The basic difference in terms of input and output voltage between (a) existing MLRs topologies and (b) proposed MLR topology.

To overcome the aforementioned constraints of conventional MLRs, a novel switched capacitors (SCs) based MLR topology is developed. The difference between the present and proposed work with input AC and output DC voltage is depicted in Fig. 2.

The power electronics interfaces for EV charging systems can support batteries ranging from 48V (e-bikes) to 400V (PHEV) [17], with the ability to charge the battery in both constant current and constant voltage modes, depending on the battery's state-of-charge (SOC). A bidirectional conventional

multilevel PFC converter operates in boost mode for charging (i.e., rectifier) and buck mode for discharging (i.e., inverter). For G2V application power need to flow from high AC grid voltage to low DC battery voltage. So, in the first stage of EV charging, there is no need to use a boost AC-DC rectifier. Moreover, for V2G, low EV battery voltage connects with high AC grid voltage. In that instant also, there is no need to use a buck inverter. This use is responsible for the requirement of a high voltage step-up and step-down DC-DC converter and high voltage DC-bus capacitor. A power flow of V2G enabled EV charging system with conventional and proposed PFC rectifier shown in Fig.3.

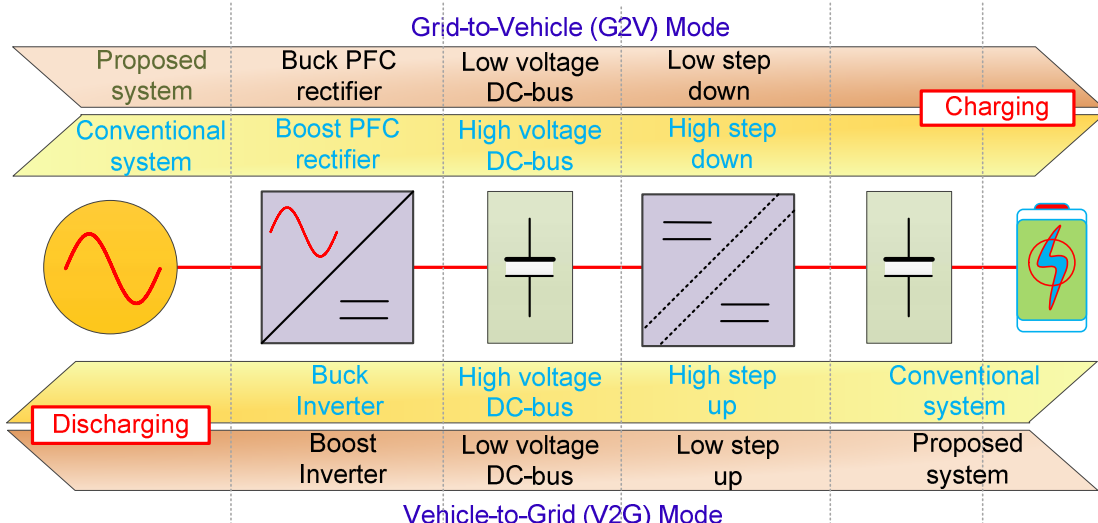


Fig. 3: Basic power flow in V2G enabled charging system and comparative effects on conventional and proposed AC-DC rectifier.

This article proposed a novel topology with the following properties to address these concerns for PFC rectifiers:

- It achieves a unity power factor and works as a V2G and G2V application.
- On the input side, it synthesizes seven levels, greatly increasing the harmonic profile.
- Ten switches, two switched capacitors, and one DC link capacitor is required.
- There is a need to balance only one DC-link capacitor voltage, the others are balanced by themselves without the use of complicated controlling methods.
- It operates in buck mode, giving it a wide output range.
- It works in continuous conduction mode (CCM), which means no huge filters are required.
- Six of ten switches have low peak inverse voltages that are the same as the DC-link voltage, and four switches have peak inverse voltages that are three times the DC-link voltage.

The proposed topology, voltage and current controller, and level-shifted pulse-width modulation (LSPWM) approach for producing gate pulses are all described in great depth. To verify the suggested work, experimental testing is carried out under steady-state and transient conditions.

Proposed buck rectifier topology

The seven-level bidirectional buck rectifier, as illustrated in Fig. 4, is made up of two H-bridges with two additional switches that link to two capacitors. By switching, connecting the two capacitors C_1 and C_2 in parallel and/or series with the DC bus capacitor represents the charging and discharging states. The operations '1' and '0' denote the ON and OFF states of the relevant switch, respectively; 'C' and 'D' represent the charging and discharging states of the capacitors are shown in Table I.

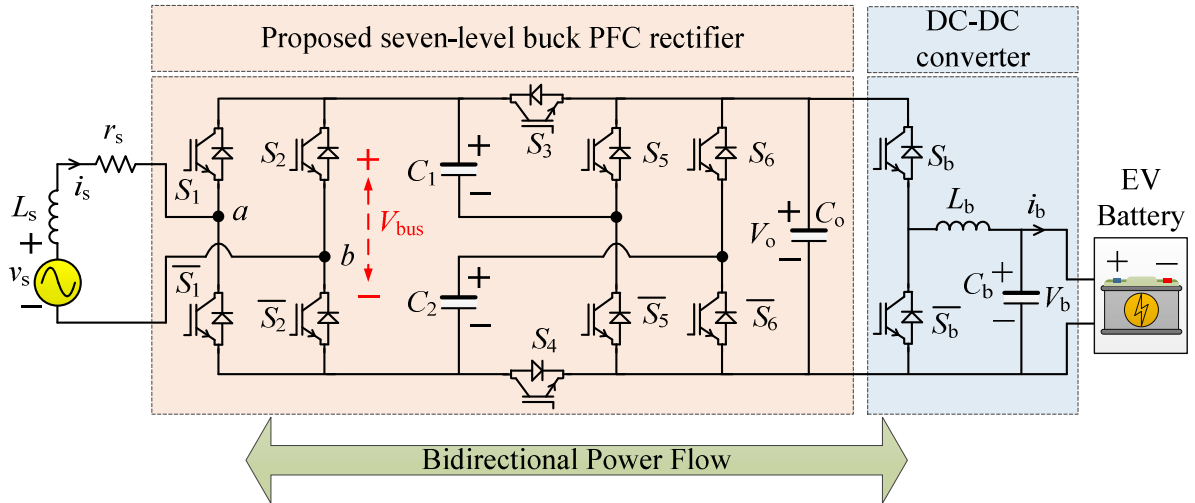


Fig. 4: Seven-level buck PFC topology for bidirectional power flow

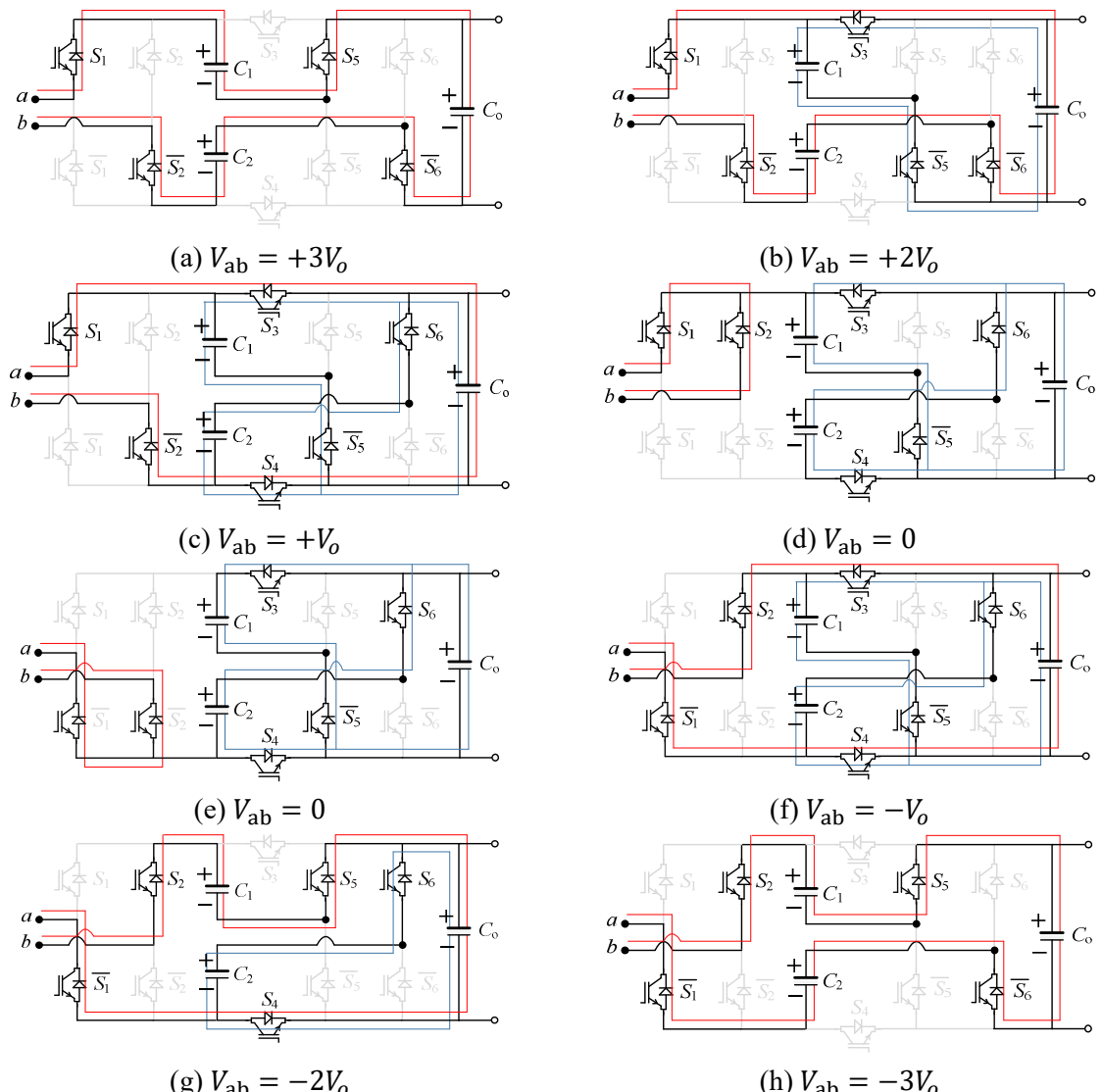


Fig. 5: Different switching states for the proposed topology

Table I: Switching states for the proposed topology

State	i_s	V_{ab}	Switches						Capacitors		
			S_1	S_2	S_3	S_4	S_5	S_6	C_1	C_2	C_o
T ₁	$i_s > 0$	$+3V_o$	1	0	0	0	1	0	C	C	C
T ₂	$i_s > 0$	$+2V_o$	1	0	1	0	0	0	D	C	C
T ₃	$i_s > 0$	$+V_o$	1	0	1	1	0	1	D	D	C
T ₄	$i_s \geq 0$	0	1	1	1	1	0	1	D	D	D
T ₅	$i_s \leq 0$	0	0	0	1	1	0	1	D	D	D
T ₆	$i_s < 0$	$-V_o$	0	1	1	1	0	1	D	D	C
T ₇	$i_s < 0$	$-2V_o$	0	1	0	1	1	1	C	D	C
T ₈	$i_s < 0$	$-3V_o$	0	1	0	0	1	0	C	C	C

The front-side H-bridge comprises four transistors S_1 , $\overline{S_1}$, S_2 and $\overline{S_2}$ are responsible for converting AC to inverted multilevel voltage. Because the bus voltage V_{bus} can be three distinct DC levels of $+V_o$, $+2V_o$, and $+3V_o$, the front-side H-bridge can create seven different voltage levels at the terminals “a” and “b” that represents as V_{ab} , namely 0 , $\pm V_o$, $\pm 2V_o$, and $\pm 3V_o$. This H-bridge has voltage stress of $3V_o$. The load-side of the seven-level rectifier has two essential features. One advantage is that all components can bear the same low voltage stress V_o , which is advantageous for high-frequency operation. Another difference is that the two capacitors C_1 and C_2 perform the same function to create distinct output levels and balance the same voltage $+V_o$ (i.e., $V_{C_1} = V_{C_2} = V_o$).

Various switching states for the proposed rectifier are described herewith:

1. **State T₁ and T₈ ($V_{ab} = \pm 3V_o$):** During this state, in the positive half cycle, the switches S_1 , $\overline{S_2}$, S_5 and $\overline{S_6}$ are turned ON. In the path shown in red, it can be seen that the capacitors C_1 , C_2 and C_o are in series with the AC source, such that the voltage $V_{ab} = (+V_{C_1} + V_{C_2} + V_o) = +3V_o$. Moreover, during the negative half cycle, the switches $\overline{S_1}$, S_2 , S_5 and $\overline{S_6}$ are turned ON, such that $V_{ab} = (-V_{C_1} - V_{C_2} - V_o) = -3V_o$. In both states, all capacitors are charged as shown in Fig. 5(a) and 5(h).
2. **State T₂ and T₇ ($V_{ab} = \pm 2V_o$):** During this state, in the positive half cycle, the switches S_1 , $\overline{S_2}$, S_3 , $\overline{S_5}$ and $\overline{S_6}$ are turned ON. In the path shown in red, it can be seen that the capacitors C_2 and C_o are in series with the AC source, such that the voltage $V_{ab} = (+V_{C_2} + V_o) = +2V_o$. Moreover, during the negative half cycle, the switches $\overline{S_1}$, S_2 , S_5 and S_6 are turned ON, such that $V_{ab} = (-V_{C_1} + V_o) = -2V_o$. In-state T₂ capacitors C_2 and C_o are charged and C_1 is discharged to the load. Furthermore, in-state T₇, C_1 and C_o are charged and C_2 is discharged. Discharging path is shown in blue as shown in Fig. 5(b) and 5(g).
3. **State T₃ and T₆ ($V_{ab} = \pm V_o$):** During this state, in the positive half cycle, the switches S_1 , $\overline{S_2}$, S_3 , S_4 , $\overline{S_5}$ and S_6 are turned ON. In the path shown with red, it can be seen that the capacitors C_o is in series with the AC source, such that the voltage $V_{ab} = +V_o$. Moreover, during the negative half cycle, the switches $\overline{S_1}$, S_2 , S_3 , S_4 , $\overline{S_5}$ and S_6 are turned ON, such that $V_{ab} = -V_o$. In states T₂ and T₇ capacitors C_o charged and C_1 , and C_2 are discharged to the load as shown in Fig. 5(c) and 5(f).
4. **State T₄ and T₅ ($V_{ab} = 0$):** During this state, in the positive half cycle, the switches S_1 , S_2 , S_3 , S_4 , $\overline{S_5}$ and S_6 are turned ON. In the path shown in red, it can be seen that not any capacitors are in series with the AC source, such that the voltage $V_{ab} = 0$. Moreover, during the negative half cycle, the switches $\overline{S_1}$, $\overline{S_2}$, S_3 , S_4 , $\overline{S_5}$ and S_6 are turned ON, such that $V_{ab} = 0$. In states T₄ and T₅ all capacitors are self-balanced and discharged to the load as depicted in Fig. 5(d) and 5(e).

The modulation approach for generating the gate pulses for the switches and the reference signal created by a suitable controller is detailed in the next section.

Modulation scheme and suitable controller

Several modulation approaches, such as multicarrier PWM and space vector modulation, can be utilized to control the output voltage of the proposed MLR. The proposed MLR is demonstrated in this part using the level shifted-PWM (LSPWM) approach, as seen in Fig. 6(a). Four high-frequency level-shifted carrier signals and reference signals produced by the controller were employed in the single-phase [18].

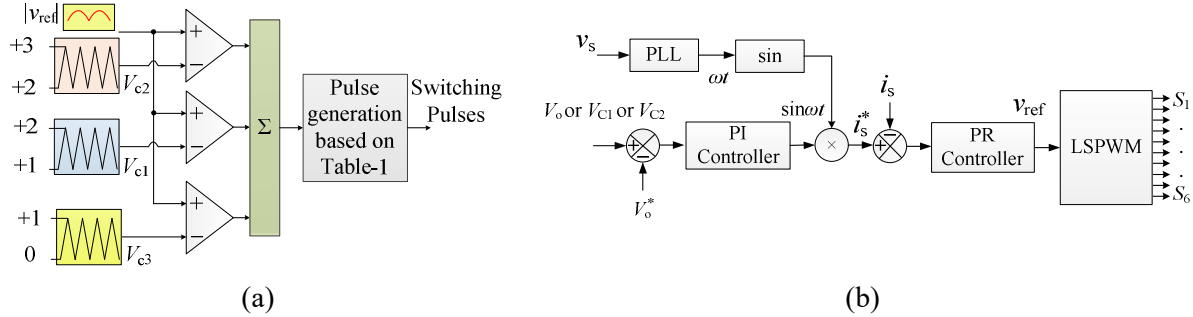


Fig. 6: Modulation and control strategy (a) level-shifted pulse width modulation for generating switching pulses (b) output voltage and PFC controller

In the proposed system cascaded PI and PR controllers are respectively used to control the DC voltage output (V_o) and the grid current (i_s), thereby providing a regulated buck DC output voltage and unity power factor at the input side. The key benefit of this proposed SC-based rectifier is that control of any one of the capacitor voltages automatically balances the voltages of the remaining capacitors. The block diagram of the implemented controller is shown in Fig. 6(b). A phase-lock loop (PLL) extracts the voltage angle and generates the synchronized current reference. The outer loop of the cascaded controller is used to regulate the voltage whose output goes to the current controller (inner loop) as the reference signal. Using the PI controller, DC voltages across the capacitors are regulated to DC voltage reference (V_o^*) [16], [19]. The current controller can be a simple gain proportional controller or a proportional-integral (PI) controller, with the inner loop having a faster dynamic than the outer loop. As a result, when using a PI controller to manage a sinusoidal input current signal, the PI's integral gain should be small enough not to affect the inner loop's speed. However, when a PI compensator is applied to a sinusoidal signal, it causes steady-state errors that appear as a DC component in the current harmonic spectrum. One approach for such a situation is to use a proportional resonant (PR) controller with an infinite gain at the fundamental grid frequency.

Experimental results

A laboratory setup was established using discrete power switches MOSFETs and a suitable gate driver IC to assess the proposed buck rectifier and closed-loop control. The output voltage and input current are sensed using a Hall Effect-based voltage sensor and current sensor. The MOSFET gate pulses are generated by the OPAL-RT OP4510, which interfaces to the hardware through MATLAB/ Simulink on the host computer. A 10-microsecond sample time is used to construct the controller and switching mechanism. A single-phase 230V RMS AC input is employed in buck mode, with 120V as a DC output. Table II summarizes the experimental verification parameters. Experimental results are taken for the resistive load and battery. Both steady-state and dynamic situations are used to evaluate the system's performance. A sudden shift in resistive DC load, reference voltage and grid voltage are examples of operating condition variations. Moreover, sudden change in battery performance from charging (i.e., G2V) to discharging mode (i.e., V2G).

The experimental results are based on two scenarios: one with an EV battery and another with resistive load. The steady-state results are produced when the rectifier converts 325V single-phase peak AC to 120V DC (in buck mode) and is further connected to the DC-DC buck converter to the EV battery. Fig. 7 shows the steady-state condition when the battery is in charging condition. Whereas, a seven-level

voltage (V_{ab}) is generated at the point of the input terminal of the rectifier, the bus voltage (V_{bus}), and all other capacitors voltages.

Table II: Parameters for experimental verifications

Parameters	Value	Unit
Single-phase input voltage	230	V (RMS)
Input grid frequency	50	Hz
Filter inductor	4	mH
Capacitors	1600	μF
Switching frequency	10	kHz
DC voltage	120	V
Battery	48V, 30AH battery	

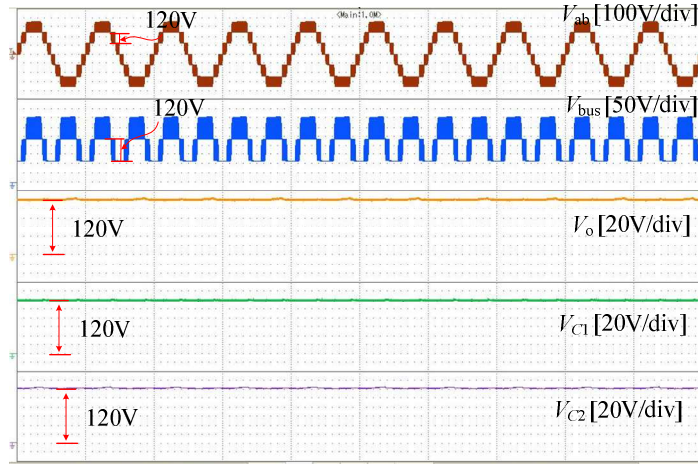


Fig. 7: Steady-state condition with level voltage (V_{ab}), bus voltage (V_{bus}) and all capacitors' voltages

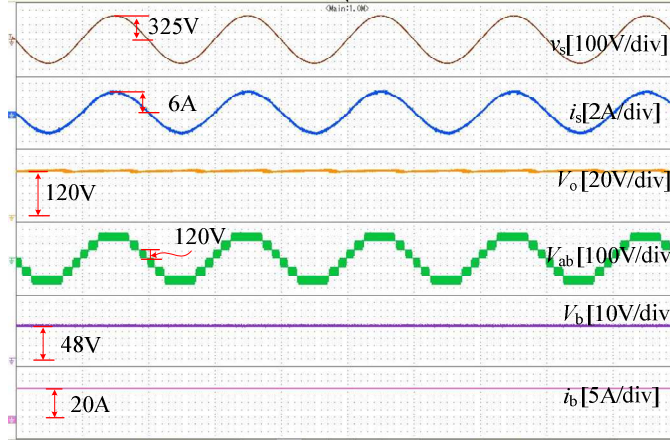


Fig. 8: Steady-state response in battery charging with unity power factor, battery voltage and current

To demonstrate applicability in single-phase charging, a power electronics interface consisting of the proposed PFC rectifier and a conventional bidirectional buck-boost DC-DC converter is built. The battery's voltage and current are 48V and 20A, respectively. Fig. 8 shows the waveforms of the battery charging, which show that the grid voltage and current are in phase. The output voltage of the rectifier is set to 120V DC and then regulated to 48V using a DC-DC converter. The V2G mode allows battery energy to be injected back into the grid. EVs can use grid-to-vehicle (G2V) charging and vehicle-to-grid (V2G) discharging modes. To use V2G mode, the interface must be capable of bidirectional power flow. In its single-phase variations, the proposed topology facilitates both charging and discharging. Experiments in both modes (G2V and V2G) of operation are shown in Fig 9. The battery current seems

to be reversed when a sudden shift in the flow of the battery current is directed. The grid current is 180° degrees out of phase with the grid voltage in this scenario.

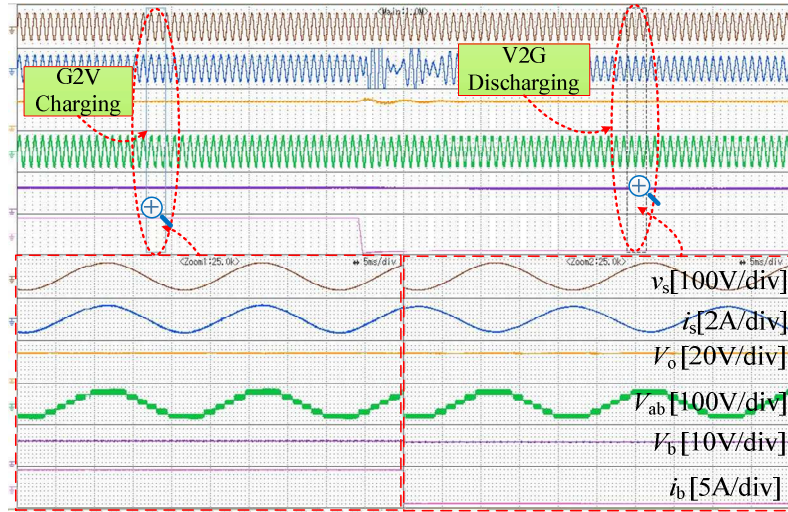


Fig. 9: Sudden change in G2V charging to V2G discharging mode

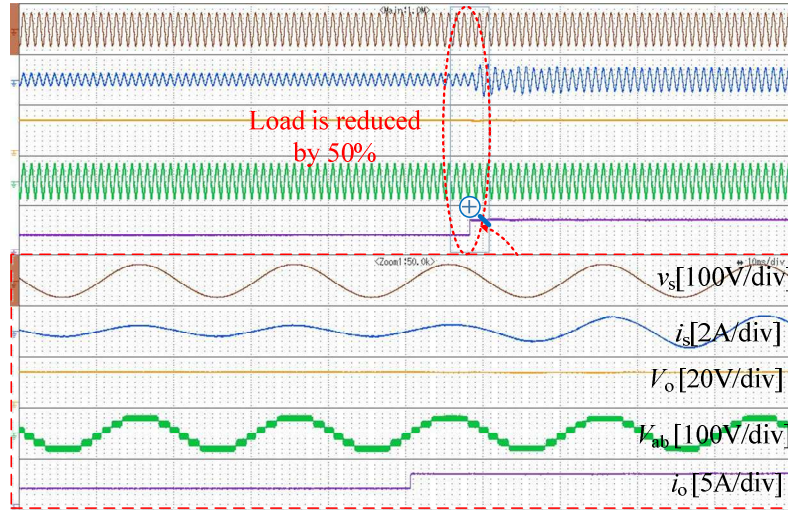


Fig. 10: Transients response with resistive load; Suddenly reduces the load by 50%

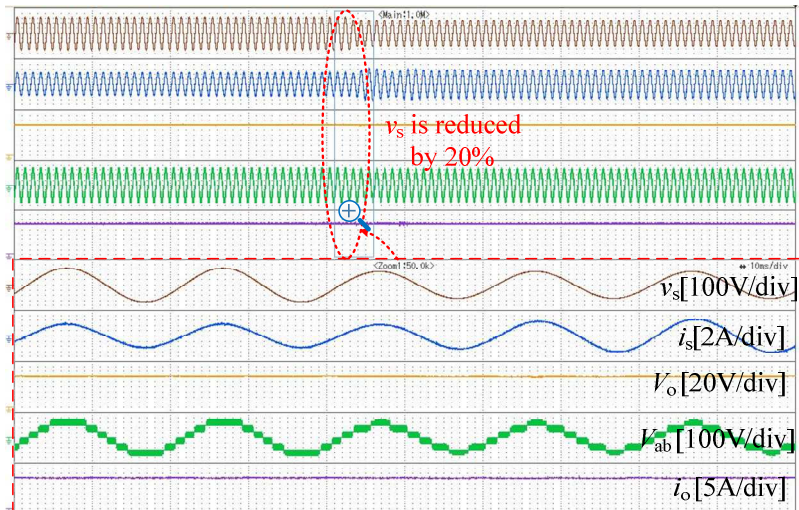


Fig. 11: Transients response with resistive load; Suddenly reduces the grid voltage by 20%

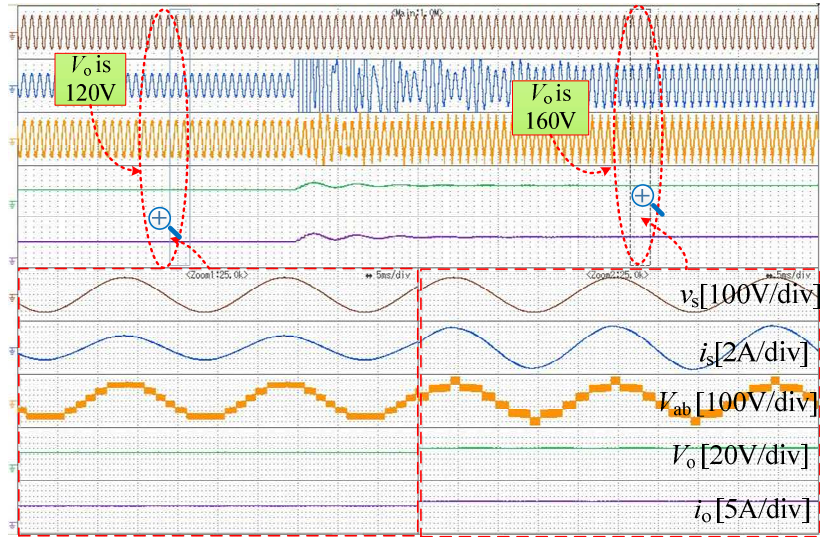


Fig. 12: Transients response with resistive load; Suddenly increases the reference voltage 120V to 160V

The proposed rectifier's dynamic performance is validated by resistive load experimentation. A 50% load rapidly decreases, as result doubling the load current and instantaneously stabilizing the load voltage at 120V. Furthermore, as seen in Fig. 10, the rectifier maintains a power factor of unity. In another case grid voltage suddenly reduces by 20% as shown in Fig. 11, as results all other voltages and currents are stable instantaneously and achieve a unity power factor. In a different case, depicted in Fig.12, if the output DC reference is increased by 120 to 160, V_o and i_o will also vary, and the load voltage will settle at 120V to 160V as expected. These outcomes validate the controller's tracking ability. The converter maintains a unity power factor and seven voltage levels at the rectifier's input even when the output voltage is raised.

Conclusion

This article presents a novel single-phase multilevel buck PFC rectifier that is most suitable for EV charging and V2G operation. LSPWM and a voltage and current controller are used to balance the voltage and maintain the unity power factor. A proto-model implementation was used to evaluate the performance on a single-phase AC input of 230 V RMS and a DC output of 120 V for various dynamic circumstances. The following conclusions were reached:

- It synthesises input into seven levels, improving the harmonic profile of the waveform.
- It offers a wide range of output voltages, making it suited for many applications.
- Because of its buck mode of operation, the proposed rectifier is appropriate for EV battery charging.
- It works in continuous conduction mode (CCM), which means no huge filters are required.
- It includes a built-in self-voltage balancing capability that eliminates the need for additional circuitry.
- It can transfer power in both directions.

References

- [1] C. C. Chan, "The state of the art of electric and hybrid vehicles," *Proceedings of the IEEE*, vol. 90, no. 2, pp. 247–275, 2002, doi: 10.1109/5.989873.
- [2] M. C. Kisacikoglu, M. Kesler, and L. M. Tolbert, "Single-phase on-board bidirectional PEV charger for V2G reactive power operation," *IEEE Transactions on Smart Grid*, vol. 6, no. 2, pp. 767–775, Mar. 2015, doi: 10.1109/TSG.2014.2360685.
- [3] V. Kumar and K. Yi, "Single-Phase, Bidirectional, 7.7 kW Totem Pole On-Board Charging/Discharging Infrastructure," *Applied Sciences*, vol. 12, no. 4, p. 2236, Feb. 2022, doi: 10.3390/app12042236.

- [4] M. C. Kisacikoglu, B. Ozpineci, and L. M. Tolbert, "EV/PHEV bidirectional charger assessment for V2G reactive power operation," *IEEE Transactions on Power Electronics*, vol. 28, no. 12, pp. 5717–5727, 2013, doi: 10.1109/TPEL.2013.2251007.
- [5] U. K. Madawala and D. J. Thrimawithana, "A bidirectional inductive power interface for electric vehicles in V2G systems," *IEEE Transactions on Industrial Electronics*, vol. 58, no. 10, pp. 4789–4796, Oct. 2011, doi: 10.1109/TIE.2011.2114312.
- [6] A. Tariq, "A Modified Battery Charger with Power Factor Correction for Plug-In Electrical Vehicles," in *The 1st International Conference on Energy, Power and Environment*, Mar. 2022, p. 103. doi: 10.3390/engproc2021012103.
- [7] D. Rothmund, T. Guillod, D. Bortis, and J. W. Kolar, "99.1% Efficient 10 kV SiC-Based Medium-Voltage ZVS Bidirectional Single-Phase PFC AC/DC Stage," *IEEE Journal of Emerging and Selected Topics in Power Electronics*, vol. 7, no. 2, pp. 779–797, Jun. 2019, doi: 10.1109/JESTPE.2018.2886140.
- [8] S. Haller, M. F. Alam, and K. Bertilsson, "Reconfigurable Battery for Charging 48 V EVs in High-Voltage Infrastructure," *Electronics (Switzerland)*, vol. 11, no. 3, Feb. 2022, doi: 10.3390/electronics11030353.
- [9] J. S. Lee, U. M. Choi, and K. B. Lee, "Comparison of tolerance controls for open-switch fault in a grid-connected T-type rectifier," *IEEE Transactions on Power Electronics*, vol. 30, no. 10, pp. 5810–5820, Oct. 2015, doi: 10.1109/TPEL.2014.2369414.
- [10] T. B. Soeiro, T. Friedli, and J. W. Kolar, "Swiss rectifier - A novel three-phase buck-type PFC topology for Electric Vehicle battery charging," in *Conference Proceedings - IEEE Applied Power Electronics Conference and Exposition - APEC*, 2012, pp. 2617–2624. doi: 10.1109/APEC.2012.6166192.
- [11] X. Xie, C. Zhao, L. Zheng, and S. Liu, "An improved buck PFC converter with high power factor," *IEEE Transactions on Power Electronics*, vol. 28, no. 5, pp. 2277–2284, 2013, doi: 10.1109/TPEL.2012.2214060.
- [12] H. Choi, "Interleaved boundary conduction mode (BCM) buck power factor correction (PFC) converter," *IEEE Transactions on Power Electronics*, vol. 28, no. 6, pp. 2629–2634, 2013, doi: 10.1109/TPEL.2012.2222930.
- [13] X. Wu, J. Yang, J. Zhang, and Z. Qian, "Variable on-time (VOT)-controlled critical conduction mode buck PFC converter for high-input AC/DC HB-LED lighting applications," *IEEE Transactions on Power Electronics*, vol. 27, no. 11, pp. 4530–4539, 2012, doi: 10.1109/TPEL.2011.2169812.
- [14] C. A. Teixeira, D. G. Holmes, and B. P. McGrath, "Single-phase semi-bridge five-level flying-capacitor rectifier," in *IEEE Transactions on Industry Applications*, 2013, vol. 49, no. 5, pp. 2158–2166. doi: 10.1109/TIA.2013.2258877.
- [15] Y. Xu, Y. Zou, C. Wang, W. Chen, and B. Liu, "A Single-Phase High-Power-Factor Neutral-pointer Clamped Multilevel Rectifier," 2007.
- [16] H. Vahedi, P. A. Labbe, and K. Al-Haddad, "Single-Phase Single-Switch Vienna Rectifier as Electric Vehicle PFC Battery Charger," Dec. 2015. doi: 10.1109/VPPC.2015.7353019.
- [17] H. Ramakrishnan and J. Rangaraju, "Power Topology Considerations for Electric Vehicle Charging Stations," 2020. [Online]. Available: www.ti.com
- [18] M. P. Kazmierkowski and L. Malesani, "Current control techniques for three-phase voltage-source pwm converters: A survey," *IEEE Transactions on Industrial Electronics*, vol. 45, no. 5, pp. 691–703, 1998, doi: 10.1109/41.720325.
- [19] D. F. Cortez and I. Barbi, "A Three-Phase Multilevel Hybrid Switched-Capacitor PWM PFC Rectifier for High-Voltage-Gain Applications," *IEEE Transactions on Power Electronics*, vol. 31, no. 5, pp. 3495–3505, May 2016, doi: 10.1109/TPEL.2015.2467210.